High-pressure magnetism of the double perovskite Sr_2FeOsO_6 studied by synchrotron ^{57}Fe Mössbauer spectroscopy

Peter Adler,[1,*] Sergey A. Medvedev,[1] Pavel G. Naumov,[1,2] Shrikant Mohitkar,[1] Rudolf Rüffer,[3] Martin Jansen,[1] and Claudia Felser[1]

[1]*Max Planck Institute for Chemical Physics of Solids, D-01187 Dresden, Germany*

[2]*Shubnikov Institute of Crystallography of Federal Scientific Research Centre "Crystallography and Photonics" of Russian Academy of Sciences, Moscow 119333, Russia*

[3]*European Synchrotron Radiation Facility, CS 40220, F-38043 Grenoble Cedex 9, France*

(Received 21 February 2019; revised manuscript received 5 April 2019; published 29 April 2019)

The pressure dependence of the magnetism of the double perovskite Sr_2FeOsO_6 was investigated by temperature- and magnetic-field-dependent synchrotron ^{57}Fe Mössbauer spectroscopy in the energy domain up to ~50 GPa. Sr_2FeOsO_6 is known to feature antiferromagnetic ordering below $T_N \sim 140$ K and a change in spin structure from AF1 to AF2 near 70 K at ambient pressure. Previous Os $L_{2,3}$ x-ray magnetic circular dichroism (XMCD) spectra [Veiga *et al.*, Phys. Rev. B **91**, 235135 (2015)] indicated a pressure-driven change from the antiferromagnetic to the ferrimagnetic state. Raman spectra of Sr_2FeOsO_6 collected at room temperature and up to 34 GPa are in agreement with previous x-ray-diffraction studies which verified that the tetragonal ambient pressure crystal structure is retained at high pressure. The Mössbauer investigations show that the Fe ions remain in the +3 high-spin ($t_{2g}^3 e_g^2$) state over the whole pressure range. The magnetic ordering is strongly stabilized by high pressure and for $p > 30$ GPa the ordering temperature is increased to above room temperature. Broad magnetic hyperfine patterns as well as coexistence of magnetic and paramagnetic signals at high pressures indicate the formation of inhomogeneous magnetic states. The shapes of applied-field Mössbauer spectra at low temperature are similar at 2 and 33 GPa and do not allow resolution of distinct antiferromagnetic and ferrimagnetic components. Pressure-induced spin canting in a basically antiferromagnetic spin structure or magnetic phase separation involving a pressure-induced minority ferrimagnetic phase may be the origin for the ferromagnetic XMCD signal.

DOI: 10.1103/PhysRevB.99.134443

I. INTRODUCTION

Applying pressure is a clean way of inducing electronic and magnetic phase transitions without disturbing impurity potentials as associated with chemical substitution [1]. High-pressure studies are particularly useful for exploring electronic and magnetic properties of correlated electronic materials which frequently depend on a peculiar balance of competing interactions with comparable energy scales involving charge, lattice, spin, and orbital degrees of freedom. However, the number of methods which allow one to study magnetism at pressures up to the megabar regime is limited. Namely, neutron experiments which are the most important tool to establish magnetic structures and excitations are still challenging at very high pressures [2].

Mössbauer spectroscopy is a powerful technique to study electronic and magnetic phase transitions at high pressure if a compound contains a suitable Mössbauer isotope. In particular ^{57}Fe Mössbauer experiments on iron-containing compounds using diamond-anvil cell (DAC) techniques have led to unique insights into electronic and magnetic transitions at pressures up to and beyond the megabar region. Examples include pressure-driven spin-state transitions in iron-based oxides with iron in different oxidation states [3–7], pressure-induced Mott transitions [8], and suppression of charge-disproportionation/ordering states [9,10], pressure-induced magnetic structure changes in negative-charge-transfer energy ferrates [11,12] as well as pressure studies probing the role of magnetism in iron-based superconductors and their relatives [13,14]. Also, high pressure properties of noniron compounds, for instance valence transitions in europium-based-compounds [15,16] or the high-pressure magnetic properties of the prototypical Mott insulator NiO [17], have been explored. Laboratory Mössbauer experiments under low-temperature and high-pressure conditions are rather time-consuming and require a sophisticated experimental setup [18]. Such experiments benefit greatly from the synchrotron variants of Mössbauer spectroscopy in the time domain (nuclear forward scattering) or in the energy domain [19–25]. In particular, energy-domain Mössbauer spectroscopy using a synchrotron Mössbauer source (SMS) for the generation of the 14.4-keV radiation of ^{57}Fe [23,26] opens up new possibilities for high-pressure research. Advantages are the high brilliance of synchrotron radiation, the lack of a nonresonant background, the full linear polarization of the SMS, and the possibility to evaluate the spectra in a similar way as conventional Mössbauer spectra which is important in materials as well as in earth science, where often complex spectra with several iron sites are encountered [27–30]. Typical data

*adler@cpfs.mpg.de

collection times are reduced from the order of days to the order of hours, which allows a much more detailed exploration of electronic and magnetic phase diagrams under pressure than in conventional experiments. A further advantage is the possibility to conveniently conduct low-temperature and high-pressure Mössbauer spectroscopy experiments in external magnetic fields, which together with the polarization of the SMS may yield more detailed insights into spin structures at high pressures. Such experiments are difficult under laboratory conditions and rarely performed [31].

An interesting class of magnetic materials are double perovskite oxides $A_2BB'O_6$ [32], where A is an alkali, alkaline earth, or rare-earth ion and B and B' are combinations of magnetic or magnetic and nonmagnetic metal ions ordered in a rocksaltlike manner. In particular, combinations of 3d and 4d or 5d transition-metal ions often lead to peculiar magnetic and magnetoelectronic properties due to the coexistence of strongly and less-correlated electronic systems and due to pronounced spin-orbit coupling which introduces a large magnetocrystalline anisotropy. Remarkable magnetic properties realized in double perovskite oxides include half metallicity with giant magnetoresistance effects [33], ferrimagnetism with high Curie temperatures [34], complex ordering patterns of the individual magnetic sublattices [35,36], the field-driven transition from a noncollinear spin structure to a Dirac ferromagnetic insulating state [37], and giant coercivity [38]. Since the double perovskite structure can be considered as two interpenetrating fcc-like lattices, a large number of exchange interactions within and between the lattices is possible, which is a source of frustration that leads to different possible magnetic structures of comparable energy. Thus, changes in the transition-metal ions as well as magnetostructural correlations induced, e.g., by chemical substitution at the A site of the perovskite structure can be used to tune the magnetic properties. For instance, Sr_2CrOsO_6 shows ferrimagnetism with an exceptionally high Curie temperature of 720 K [34], whereas the iron counterpart Sr_2FeOsO_6 reveals antiferromagnetic order below 140 K and features a spin structure change near 70 K [39]. On the other hand, the calcium analogs Ca_2CrOsO_6 [40] and Ca_2FeOsO_6 [41] both are ferrimagnets with T_C's of 490 and 320 K, respectively. In case of the iron compounds, cationic substitution at the A site not only induces a structural change from a tetragonal (space group $I4/m$ for $A = Sr$) to a monoclinic (space group $P2_1/n$ for $A = Ca$) crystal structure but also a change from an antiferromagnetic to a ferrimagnetic spin structure. This has been explained in terms of a weakening of ferromagnetic σ-type exchange interactions between the half-filled and empty e_g orbitals of the 3d and the 5d transition-metal ions due to octahedral tilting in Ca_2FeOsO_6 [42,43]. The barium-analog Ba_2FeOsO_6 reveals ferrimagnetism above room temperature too, but adopts the hexagonal perovskite structure [44].

It has been demonstrated by Veiga *et al.* that not only cationic substitution but also high pressure modifies the magnetic properties of Sr_2FeOsO_6 [42]. Using x-ray magnetic circular dichroism (XMCD) spectroscopy at the Os $L_{2,3}$ edge up to 40 GPa at 15 K, the continuous evolution of a ferromagnetic signal with increasing pressure was found, which, however at 40 GPa is still only about 40% of that of Ca_2FeOsO_6 at ambient pressure. Most remarkably, the crystal structure of Sr_2FeOsO_6 remained tetragonal up to 56 GPa. It was suggested that high pressure induces a transition to the ferrimagnetic state by increasing the crystal-field splitting at Os^{5+} sites rather than by bending of the Fe–O–Os bonds [42]. The XMCD experiments at high pressure only probed the Os site, and details of the temperature dependence of the magnetic transitions were not derived. Here, we report a detailed investigation of the high-pressure magnetism of Sr_2FeOsO_6 by energy-domain synchrotron ^{57}Fe Mössbauer spectroscopy up to about 50 GPa. In order to get insights into the nature of the magnetic ground-state, low-temperature spectra were also recorded in applied fields up to 6 T; further on, Raman spectra up to 34 GPa were obtained. Our data show that at high pressure an inhomogeneous magnetic state is formed which reflects the various competing exchange pathways in this system. The magnetic ordering temperature increases strongly with pressure, while the type of magnetic ordering at high pressure cannot be clarified unambiguously from powder spectra.

II. EXPERIMENTAL DETAILS

Sr_2FeOsO_6 enriched with 20% ^{57}Fe was synthesized as polycrystalline powder from stoichiometric amounts of binary oxides at 1243 K in an evacuated sealed quartz ampule in analogy to Ref. [45]. The reagent SrO_2 (Sigma Aldrich, 99%) was used as received; Fe_2O_3 (enriched with 20% ^{57}Fe) was prepared from a mixture containing 20% of iron-57 powder and 80% iron powder with normal isotopic abundance; see Supplemental Material, Ref. [46] for details. Purchased OsO_2 (Sigma Aldrich, 83% Os) contained ~30% of osmium metal and was therefore oxidized by heating in the presence of a stoichiometric amount of PbO_2 at 753 K in an evacuated sealed quartz ampule to get highly pure OsO_2. The starting mixture containing stoichiometric amounts of SrO_2 (120 mg), Fe_2O_3 (20% ^{57}Fe, 40 mg), and OsO_2 (112 mg) was ground thoroughly inside a glovebox and pressed into a pellet that was placed in a corundum container and finally sealed in an evacuated quartz ampule of approximately 2-cm diameter and 15-cm length. Pure single-phase polycrystalline Sr_2FeOsO_6 (20% ^{57}Fe) was obtained after heating for 48 h at 1243 K. The heating and cooling rates were kept at 50 K/h throughout.

The purity of the sample was checked by powder x-ray diffraction using a Huber G670 camera [Guinier technique, $\lambda = 1.788\,92$ Å ($CoK_{\alpha 1}$)].

Mössbauer spectra at ambient pressure were collected with a conventional WISSEL Mössbauer spectrometer which was operated in constant acceleration mode and used a ^{57}Co/Rh radioactive source. A few milligrams of iron-57 enriched Sr_2FeOsO_6 was diluted with boron nitride in order to ensure homogeneous distribution in a Plexiglas sample container which was placed inside a JANIS SHI-850-5 closed-cycle refrigerator. The spectra were evaluated with the program MOSSWINN [47].

Energy-domain Mössbauer spectra at high pressures up to about 50 GPa were conducted between 3 and 295 K in diamond-anvil cells using the synchrotron Mössbauer source at the nuclear resonance beamline ID18 of the European Synchrotron Radiation Facility (ESRF, Grenoble) for the generation of the 14.4-keV radiation [26]. For generation of high

pressure, DACs manufactured from the nonmagnetic alloy MP35N and equipped with Boehler-Almax design, diamond anvils with 500-μm culets were used. The powdered sample was loaded into a sample chamber of 200-μm diameter which was obtained by preindenting a cavity of 40-μm thickness into the tungsten gasket. Silicone oil was used as pressure-transmitting medium. The pressure was determined by the ruby luminescence method. The DACs were placed into a cryomagnetic system from CryoIndustries. The beam size of the SMS radiation was 9 μ (vertical) and 16 μ (horizontal), respectively. The velocity scale was calibrated with a 25-μ α-iron foil and the linewidth and center shift of the SMS were determined by measuring repeatedly the spectra of the single-line absorber $K_2Mg^{57}Fe(CN)_6$ having an intrinsic linewidth of 0.21 mm/s. The data analysis was performed by using the transmission integral and a version of the program MOSSWINN where a squared Lorentzian for describing the line shape of the SMS has been implemented. The source linewidth thus obtained was about $3\Gamma_0$ (Γ_0 is the natural linewidth of the 14.4-keV transition of ^{57}Fe), in agreement with previous results [26]. Most Mössbauer spectra were recorded without external magnetic field but a few spectra were collected in longitudinal magnetic fields of 3 or 6 T. All isomer shifts given in this work are referred to α-iron.

High-pressure Raman spectra at room temperature were recorded in backscattering geometry using a customary micro-Raman spectrometer with a HeNe laser as the excitation source ($\lambda = 632.8$ nm) and a single-grating spectrograph with 1-cm^{-1} resolution.

III. RESULTS AND DISCUSSION

A. Ambient-pressure characterization

For providing optimal experimental conditions in the SMS experiments we have prepared a sample of Sr_2FeOsO_6 containing 20% of ^{57}Fe, which in the following will be denoted as $Sr_2{}^{57}FeOsO_6$. The x-ray-diffraction (XRD) pattern of the $Sr_2{}^{57}FeOsO_6$ sample (Fig. S1 in Ref. [46]) could be well refined in space group $I4/m$ with lattice constants $a = 5.542(1)$ Å and $c = 7.881(1)$ Å, in agreement with earlier results [45]. No impurity peaks are detected. The analysis of the XRD pattern indicates a 4(1)% degree of Fe-Os antisite disorder. The antisite disorder is also reflected in the shape of the room-temperature Mössbauer spectrum of $Sr_2{}^{57}FeOsO_6$ which was collected in a velocity range between -4 and $+4$ mm/s [Fig. 1(a)], and which showed a broad single line with a shoulder towards lower Doppler velocities. Fitting of the spectrum by assuming a superposition of a single line and a quadrupole doublet (quadrupole splitting, QS) and using the transmission integral resulted in an isomer shift IS = 0.455(1) mm/s for the singlet and IS = 0.412(2) and QS = 0.80(1) mm/s for the doublet component. The area fractions from this fit are 86 and 14%, respectively. A weak low-energy shoulder in the room-temperature Mössbauer spectrum of Sr_2FeOsO_6 was observed previously [48] and assigned to an Fe^{4+} impurity corresponding to the $SrFeO_{3-d}$ system. In light of the present Mössbauer spectrum of $Sr_2{}^{57}FeOsO_6$ where this feature is more apparent it appears likely that also in the earlier work it rather was a manifestation of the residual antisite disorder. The observation of a single line with IS = 0.46 mm/s for the majority component is in good agreement with the previous work [39,48] and confirms that in well-ordered Sr_2FeOsO_6 the Fe atoms have a nearly cubic environment (small tetragonal distortion), whereas the minority quadrupole doublet reflects the different local environment of iron atoms in regions which are affected by antisite (AS) disorder. Each AS defect results in six structurally distorted iron atoms which are reflected in an increased quadrupole splitting. The area fraction of about 14% for the doublet component compares well with an AS defect level of a few percent. Similar features in Mössbauer spectra reflecting AS disorder were observed for other iron double perovskites, e.g., Sr_2FeReO_6 [49].

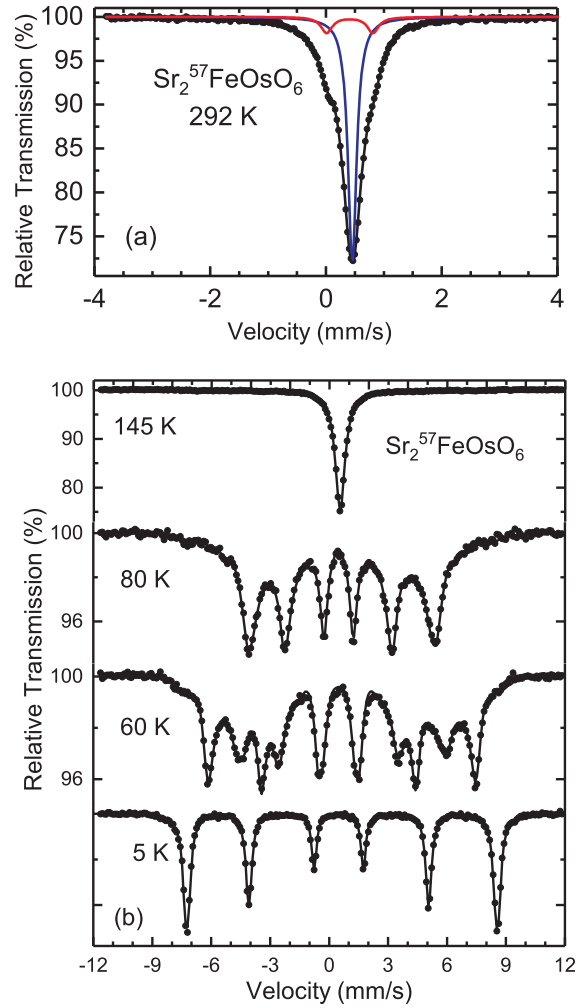

FIG. 1. Selected Mössbauer spectra of $Sr_2{}^{57}FeOsO_6$ at the indicated temperatures. (a) Mössbauer spectrum at room temperature in a restricted velocity range. The absorber function was decomposed into a single line and a quadrupole doublet with Lorentzian line shape by fitting the spectrum using the transmission integral. (b) Temperature-dependent spectra which illustrate the magnetic phase transitions of the systems near 60 and 140 K. The dots correspond to the experimental data whereas the solid lines are the calculated spectra where hyperfine-field distributions were extracted using the Hesse-Rübartsch method. Here, the thin absorber approximation was used for the data evaluation. At 145 K only a paramagnetic signal is found.

Selected Mössbauer spectra of $Sr_2{}^{57}FeOsO_6$ recorded over an extended velocity range are shown in Fig. 1(b); a more comprehensive selection of spectra is given in Fig. S2 of Ref. [46]. At 5 K a single, rather sharp hyperfine sextet with IS = 0.57 mm/s and a hyperfine field $B_{hf} = 49$ T is found which shows that all Fe atoms are fully magnetically ordered and feature the full local magnetic moment expected for Fe^{3+}. According to neutron-diffraction studies [39], the magnetic ground state of Sr_2FeOsO_6, which was labeled as AF2, features a spin alignment along the *c* direction with ferrimagnetic ordering of Fe and Os moments in the *ab* plane but an alternating up-up-down-down spin alignment along *c*. By contrast, the spectrum at 60 K shows two components, still the relatively sharp AF2 component, but in addition a much broader pattern with a peak hyperfine field of 33 T. The 60 K spectrum signals the transition from the AF2 ground state to the AF1 spin structure where the moments show ferrimagnetic alignment in the *ab* plane too, but where the moments along *c* reveal parallel spin alignment [39]. The transition occurs mainly between about 50 and 70 K in the present sample [46] and no AF2 signal is apparent anymore at 70 K and above. As in our previous study [39,48] it is apparent that the Mössbauer patterns corresponding to the AF1 phase are much broader than those of the AF2 phase and here the spectra were fitted by extracting a hyperfine-field distribution according to the model-independent Hesse-Rübartsch method assuming a single isomer shift and quadrupole splitting for each spectrum, see Fig. S2 in Ref. [46]. The transition to the paramagnetic state occurs near 140 K and the spectra at 145 K and higher temperatures can be essentially described by a single line (the low-energy shoulder is not well resolved in the large-velocity scale spectra). The temperature ranges of the magnetic transitions compare well with those in our previous work.

The broad B_{hf} distributions for the AF1 phase in the temperature range $60\,K \leqslant T \leqslant 140\,K$ suggest that below $T_N \sim 140$ K an inhomogeneous magnetic state is formed. In this temperature range reduced ordered magnetic moments *m* [39] and as $B_{hf} \sim m$ also reduced B_{hf} values compared to the typical values in Fe^{3+} compounds indicate that not all spin degrees of freedom are fully ordered yet. These observations can be considered as signs of frustration effects reflecting the competing exchange interactions in this double perovskite. The transformation to the AF2 structure below 70 K, which may be accompanied by a small structural modification [39,50], relaxes the frustration, and both the magnetic moments and the B_{hf} values are enhanced and the Mössbauer lines become sharper. Accordingly, the transition from the AF1 to the AF2 phase gives rise to an anomaly in $B_{hf}(T)$ [39,48]. This observation is somewhat reminiscent of certain reentrant spin-glass systems, where the random freezing of transverse spin components below the magnetic ordering temperature T_m was considered as the origin for a similar anomaly in $B_{hf}(T)$ [51–54]. Additional insights into the nature of the AF1 and AF2 spin structures were obtained from recent inelastic neutron-scattering studies on powder samples of Sr_2FeOsO_6 which revealed formation of a spin excitation gap only in the AF2 phase, whereas in the AF1 phase an ungapped spin excitation spectrum was obtained [50]. The latter indicates strong spin fluctuations in the AF1 phase which may be the origin for the broad Mössbauer hyperfine pattern. Resonant inelastic x-ray-scattering experiments suggested that the spin excitation gap in the AF2 phase is associated with pronounced spin-orbit coupling, which leads to a splitting of the t_{2g} manifold of states with a resulting $J = 3/2$ rather than a simple $S = 3/2$ state and a pronounced magnetocrystalline anisotropy [50].

Sr_2FeOsO_6 essentially is an atomically ordered double perovskite, but details of the magnetic transitions and Mössbauer line shapes may be influenced by the remaining AS disorder. Nevertheless, it is unlikely that the AS defect fraction of typically a few percent is the main origin for the unusual features in the magnetism of Sr_2FeOsO_6. The magnetic properties of various Sr_2FeOsO_6 samples prepared in different laboratories with different techniques agree quite well although the AS defect levels are somewhat different [45,55,56,50]. Further on, multiple magnetic phase transitions and partial order of magnetic moments were also observed in other double perovskites where AS disorder does not play a role, cf. the cases of Sr_2CoOsO_6 [35,36] and Sr_2YRuO_6 [57]. On the other hand, varying fractions of residual AF1 phase seen in neutron-diffraction patterns even at the lowest temperatures [39,50] may be related to the presence of AS defects. Mössbauer spectroscopy cannot detect whether a certain fraction of AF1 phase is also retained in the present $Sr_2{}^{57}FeOsO_6$ sample as the Fe hyperfine field is fully developed for all sites at low temperatures [39].

B. High-pressure Raman spectroscopy

To monitor the possibility of a pressure-induced structural transition, Raman spectra of our $Sr_2{}^{57}FeOsO_6$ sample were measured at room temperature up to a pressure of 34 GPa [Fig. 2(a)]. According to the XRD studies, Sr_2FeOsO_6 crystallizes in the tetragonal space group $I4/m$ for which factor-group analysis reveals nine Raman-active modes ($\Gamma_{Raman} = 3A_g + 3B_g + 3E_g$) [58]. However, as seen from the single-line Mössbauer spectra in the paramagnetic phase the distortion from the cubic structure is small at ambient pressure. Therefore, the phonon mode assignment is similar to that of cubic perovskites [58]. The cubic aristotype of the double perovskites crystallizes in space group $Fd\text{-}3m$, where group theory predicts four Raman-active modes, namely $\nu_1(A_{1g})$, $\nu_2(E_g)$, $\upsilon_5(F_{2g})$, and $T(F_{2g})$ [59]. Here, ν_1 and ν_2 correspond to the symmetric and antisymmetric stretching vibrations of the octahedra, whereas ν_5 corresponds to the oxygen bending motions. In addition, a lattice mode (T) is expected. In the Raman spectra of cubic or nearly cubic tungsten double perovskites A_2MWO_6 the A_{1g}, E_g, and T modes were observed [59], whereas for $Sr_2{}^{57}FeOsO_6$ only one strong mode occurring at $>800\,cm^{-1}$ was found [Fig. 2(a)] which can be assigned to the ν_1 symmetric stretching of OsO_6 octahedra. It should be noted that the ν_1 peak often dominates Raman spectra of distorted perovskites and the number of observed modes is significantly smaller than expected [60]. It might be possible that luminescence of diamond anvils in our experiments precludes the observation of other weak modes. No qualitative changes are observed in the Raman spectra upon increase of the pressure up to 34 GPa [Fig. 2(a)] and the

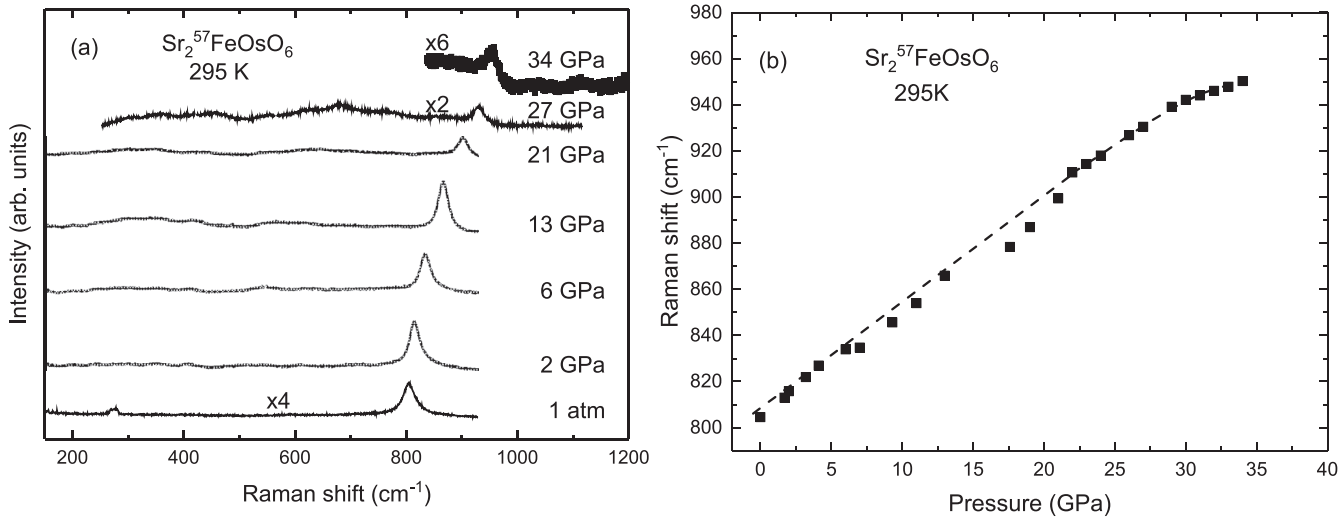

FIG. 2. (a) Raman spectra of $Sr_2{}^{57}FeOsO_6$ at the indicated pressures showing the ν_1 stretching mode. Strongly enhanced background due to luminescence of the stressed diamond anvils precludes Raman measurements up to higher pressures. (b) Pressure dependence of the frequency of the ν_1 mode. Dashed lines are guides to the eye.

pressure dependence of the ν_1 frequency shows continuous increase as pressure increases [Fig. 2(b)]. This observation indicates the structural stability of the tetragonal crystal structure of Sr_2FeOsO_6 up to the highest pressure of 34 GPa which was applied in this experiment, in full agreement with high-pressure synchrotron x-ray-diffraction studies [42].

C. High-pressure synchrotron Mössbauer spectroscopy in zero field

High-pressure Mössbauer spectra of $Sr_2{}^{57}FeOsO_6$ using the SMS were recorded in DACs up to pressures of about 50 GPa. Firstly we discuss the pressure dependence of the low-temperature spectra (at ∼3 K) which are shown in Fig. 3. In addition to the intrinsic signal from the sample, most of the spectra recorded at various pressures and temperatures revealed a weak singletlike feature (IS ∼ 0.25−0.35 mm/s) which was not present in the ambient pressure Mössbauer spectra recorded in the laboratory. This feature most likely reflects an iron impurity in the beryllium compound refractive lenses (CRLs) of the focusing optics and/or in the beryllium windows of the cryomagnet. The intensity ratios between the components of the hyperfine sextet strongly deviate from those in the laboratory spectra (cf. Figs. 1 and 3). The radiation emitted by the SMS is linearly polarized; however, in case of an arbitrary powder the spectra should not differ from those obtained with an unpolarized source. Thus, the decreased intensity of the second and fifth lines in the spectra indicates that pressurization in the DAC leads to preferred orientation of the hyperfine field parallel to the direction of the SMS beam. As the magnetic moments and accordingly the hyperfine fields in Sr_2FeOsO_6 are oriented along the tetragonal c axis, this implies that the c axis is preferentially oriented along the direction of the x-ray beam. Preferred orientation originates most likely from a uniaxial pressure component due to poor hydrostaticity of the silicon oil pressure-transmitting medium, the uniaxial character of the DAC loading procedure, and the nonspherical shape of powder grains.

Since the spectra feature a certain asymmetry, they were evaluated using two magnetic subspectra with Lorentzian line shape, assuming a common ratio of the intensities between

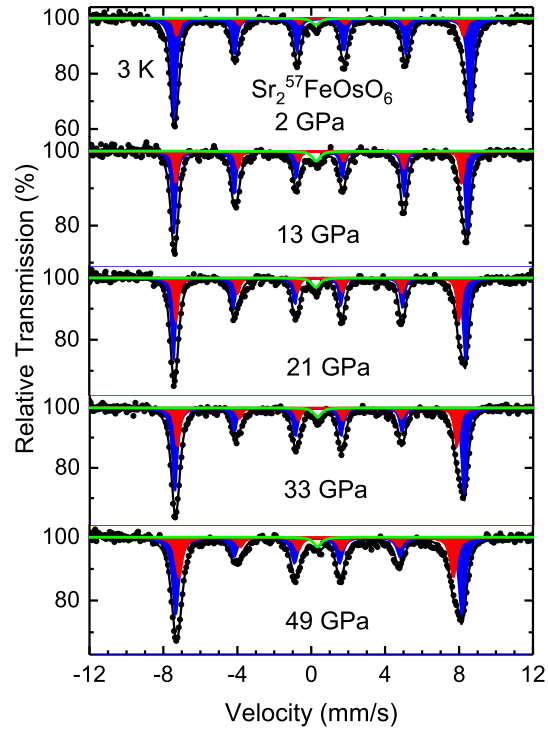

FIG. 3. SMS spectra of $Sr_2{}^{57}FeOsO_6$ at 3 K and the indicated pressures. The hyperfine pattern was decomposed into two components which are highlighted (in blue and red, respectively). The additional broad single line (green) is assigned to an Fe impurity of the beryllium CRLs of the focusing optics and/or in the windows of the cryomagnet.

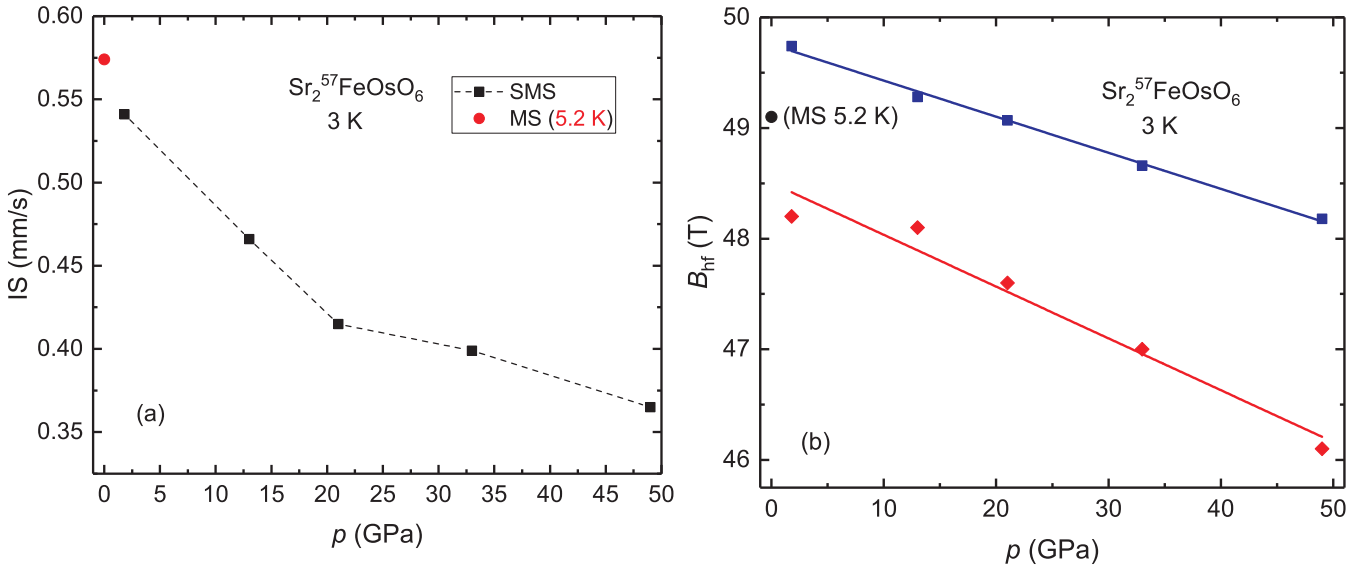

FIG. 4. Pressure dependence of (a) the isomer shift and (b) the hyperfine fields of the two subspectra (right) for $Sr_2{}^{57}FeOsO_6$ at 3 K.

lines 2 and 5 and lines 3 and 4, respectively (the latter being the inner lines) which was varied in the fits. The two components differ in their hyperfine fields as well as in their quadrupole splitting parameters, while the isomer shifts were assumed to be equal. The linewidths of the two subspectra somewhat arbitrarily were constrained to be the same. No dramatic changes occur in the spectra up to 50 GPa. All iron ions stay in a well-ordered magnetic state. The only apparent change is that the slight asymmetry in the spectra becomes more pronounced under pressure. The asymmetry in the spectra may indicate the coexistence of magnetic phases slightly differing in their hyperfine interactions. It is tempting to associate the second component in the Mössbauer spectra with the continuous evolution of the ferromagnetic component seen in the XMCD spectra [42]. However, this cannot be quantitatively corroborated as the intensity ratio between the two components in the Mössbauer spectra does not feature a clear trend with pressure which partly may be due to the fact that the poor structure of the spectra does not allow an unambiguous separation of the two subspectra. The pressure dependence of the isomer shift and of the hyperfine fields is shown in Figs. 4(a) and 4(b), respectively. The decrease of IS with pressure can be attributed to an increased *s* electron density at the nucleus in the course of the volume decrease. The overall decrease between 2 and 49 GPa by about 0.17 mm/s is comparable to that in other Fe^{3+} oxides [3]. However, the decrease in IS with p appears to be more pronounced up to 20 GPa, whereas it levels off at higher pressure. The hyperfine fields between 2 and 49 GPa decrease linearly by 1.5 and 2 T for the high-field and low-field component, respectively. Since B_{hf} can be written as $B_{hf}(p,T) = B_{hf}(p,0) \cdot F(T,T_m)$ [61], where $B_{hf}(p,0)$ corresponds to the saturation hyperfine field at a given pressure p and $F(T,T_m)$ reflects the dependence of B_{hf} on temperature T and ordering temperature T_m (T_N or T_C); the pressure dependence of B_{hf} reflects both the pressure dependence of T_m as well as the pressure dependence of $B_{hf}(p,0)$. For Sr_2FeOsO_6 the ordering temperature increases strongly with pressure, see below; thus $F(T,T_m)$ and accordingly B_{hf} is generally expected to increase with p. At 3 K, however, $B_{hf}(p, 3\,K) \approx B_{hf}(p,0)$ and the decrease in B_{hf} is attributed to a slight decrease in the iron magnetic moment due to an enhanced covalency (smaller Fe-O-Os distances) under pressure. Both the moderate pressure dependence of IS and B_{hf} confirm that the electronic structure at the Fe sites basically remains unchanged up to 50 GPa. In particular, there are no indications for a pressure-induced spin-state transition and collapse of magnetism as observed for some simple Fe^{3+} $RFeO_3$ perovskites in a similar pressure range [3,5] or for a pressure-induced charge transfer between Fe and Os orbitals. The Fe ions remain in the $+3\,t_{2g}{}^3e_g^2$ high-spin state over the entire pressure range.

By contrast, pronounced pressure-induced changes are apparent in the room-temperature SMS spectra which are depicted in Fig. 5. Whereas the spectra at pressures of 2 and 13 GPa reveal only a single signal which can be described by a quadrupole doublet, the spectra at 33 and 49 GPa show the presence of a broad magnetic hyperfine pattern in addition to a quadrupole doublet. Accordingly, the ordering temperature has increased from ~140 K at ambient pressure to above room temperature at pressures above 30 GPa, which corresponds to an average $dT_m/dp > 5\,K/GPa$. The strong enhancement of T_m under pressure supports the view that Sr_2FeOsO_6 can be considered as an electronically localized Mott-insulating electronic system [62] where the exchange interactions are enhanced due to the decrease in interatomic distances. However, the hyperfine-field distributions at room temperature, here tentatively approximated by two components with Gaussian B_{hf} distribution, are very broad, which indicates that the magnetic system is inhomogeneous. This possibly reflects a distribution in magnetic ordering temperatures and/or spin-fluctuation times. Contrary to the ambient pressure spectrum, the quadrupole doublet is resolved even at 2 GPa and there appears to be a certain increase in quadrupole splitting with pressure for the residual paramagnetic phase at room temperature, which is in agreement with the increased c/a ratio derived from the XRD data [42].

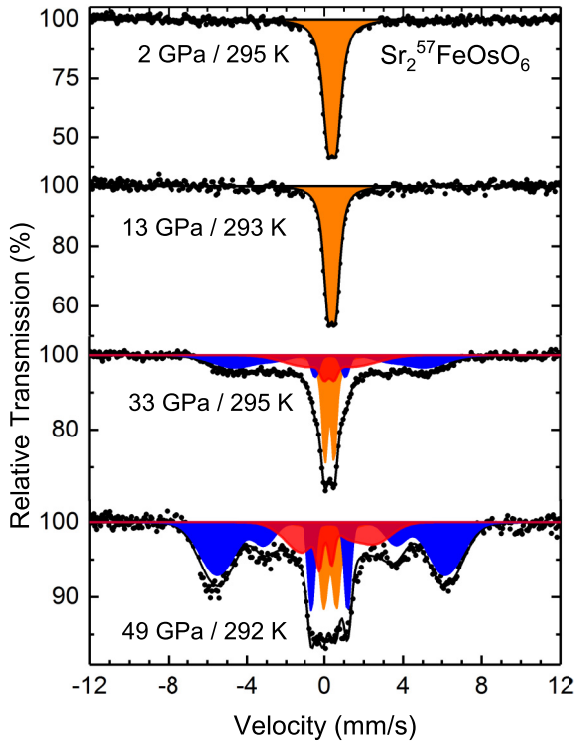

FIG. 5. SMS spectra of $Sr_2{}^{57}FeOsO_6$ near room temperature at the indicated pressures. The subspectra due to magnetic hyperfine splitting at 33 and 49 GPa were decomposed into two components which are highlighted (in blue and red, respectively).

More details about the magnetic phase transitions are obtained from the temperature dependence of the SMS spectra of $Sr_2{}^{57}FeOsO_6$ which was studied in detail at 2 and 33 GPa. Even at the relatively small pressure of 2 GPa significant changes compared to the spectra at ambient pressure are apparent (Fig. 6). Whereas at 3 K all Fe^{3+} ions are still fully ordered with $B_{hf} \sim 49.8$ T for the main component, the AF2-AF1 transition is more obscured than in the ambient pressure spectra. This is due to the fact that the B_{hf} distribution related to the AF1 phase is even broader than at ambient pressure and its average B_{hf} has increased by about 10 T. Accordingly, the AF1 and AF2 subspectra are not as well separated as at ambient pressure and partly merge together. Nevertheless, the sharper AF2 signal is still discernible up to ~90 K, indicating that the AF2 phase is somewhat stabilized under pressure. Even more remarkable is that a magnetic hyperfine pattern, although very broad, is seen up to about 220 K whereas it had completely disappeared at 145 K at 0 GPa. Above 150 K, the area fraction of the paramagnetic phase increases continuously with increasing pressure, showing that magnetically ordered and paramagnetic phase coexist over a large temperature range. These results corroborate further the peculiar properties of the AF1 phase. Obviously, even a pressure of 2 GPa is sufficient to modify the balance of competing interactions which stabilizes the AF1 phase to higher temperatures.

On the other hand, there are no pronounced changes in the SMS spectra up to 160 K at 33 GPa (Fig. 7). This demonstrates that in this pressure range all the Fe^{3+} ions essentially keep the full magnetic moment. The AF1-AF2 transition is no longer clearly discernible, but its presence cannot be ruled out. In the low-pressure regime it could only be detected as the ordered magnetic moments and thus the hyperfine fields in the two phases were different, whereas in case of similar or equal moments and for small quadrupole splitting, Mössbauer spectroscopy cannot discriminate between the two different types of antiferromagnetic spin structures. There are indications for subtle variations in the line shape above 50 K which may suggest a magnetic transition in this temperature range at 33 GPa. Compared to the spectra in the low-pressure regime the signals remain relatively sharp below ~160 K. Only for $T > 160$ K significant broadening of the hyperfine pattern sets in and a paramagnetic signal evolves, the area fraction of which increases continuously with increasing

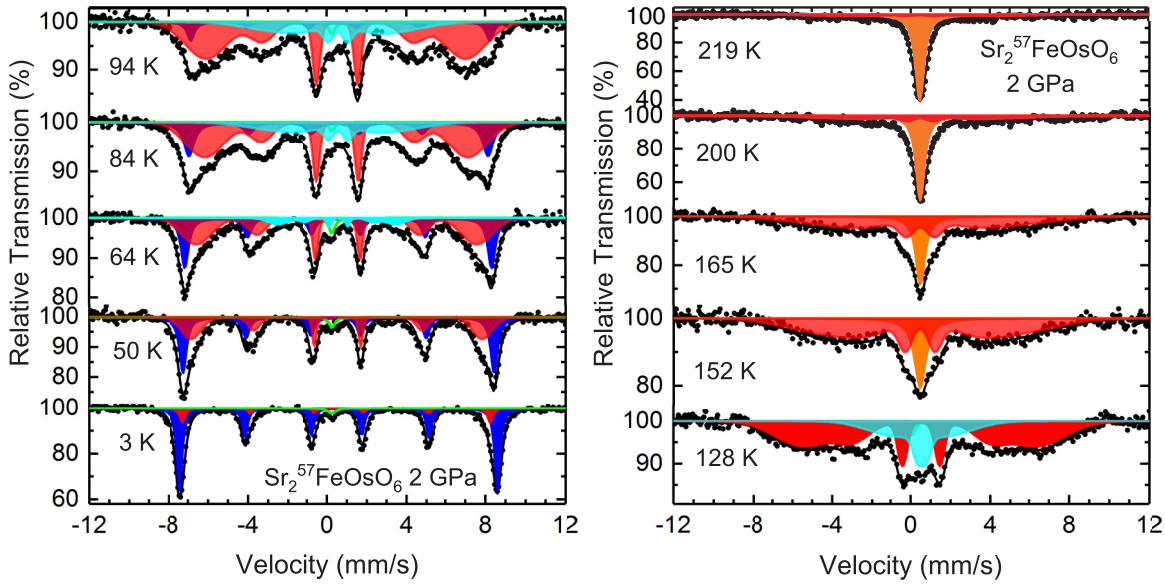

FIG. 6. Temperature dependence of the SMS spectra of $Sr_2{}^{57}FeOsO_6$ at 2 GPa. The decomposition of the spectra into components is highlighted.

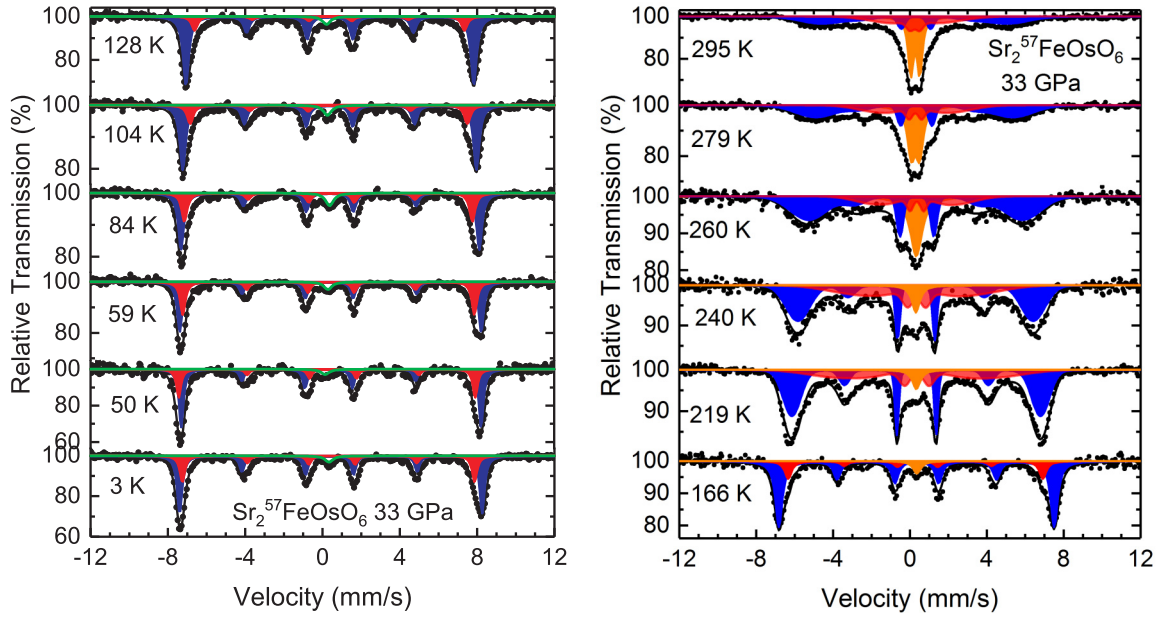

FIG. 7. Temperature dependence of the SMS spectra of $Sr_2{}^{57}FeOsO_6$ at 33 GPa. The decomposition of the spectra into components is highlighted.

temperature. At 33 GPa and room temperature still about two-thirds of the sample are in the magnetically ordered state. Again, these observations suggest a strongly inhomogeneous magnetic state with a distribution of ordering temperatures and the presence of spin fluctuations. At 49 GPa even more than 80% of the material is in the magnetically ordered state at room temperature.

D. High-pressure synchrotron Mössbauer spectroscopy in applied magnetic fields

From the previous XMCD study it was suggested that Sr_2FeOsO_6 undergoes a pressure-driven change from the antiferro- to the ferrimagnetic spin structure [42]. A unique feature of the SMS is that it conveniently allows one to collect Mössbauer spectra under low-temperature/high-pressure conditions in external magnetic fields which potentially provide additional information on spin structures. We have collected low-temperature spectra of $Sr_2{}^{57}FeOsO_6$ at 2 and 33 GPa in longitudinal magnetic fields of 3 and 6 T (Fig. 8). The main observation is a broadening of the spectra with increasing external field B_{ext} at both pressures. In order to describe the broadening more quantitatively, we have fitted the spectra by a single magnetic component with a Gaussian distribution of hyperfine fields, here neglecting the asymmetry in the spectra. Actually improved fits are obtained using two magnetic components but due to the poor structure of the

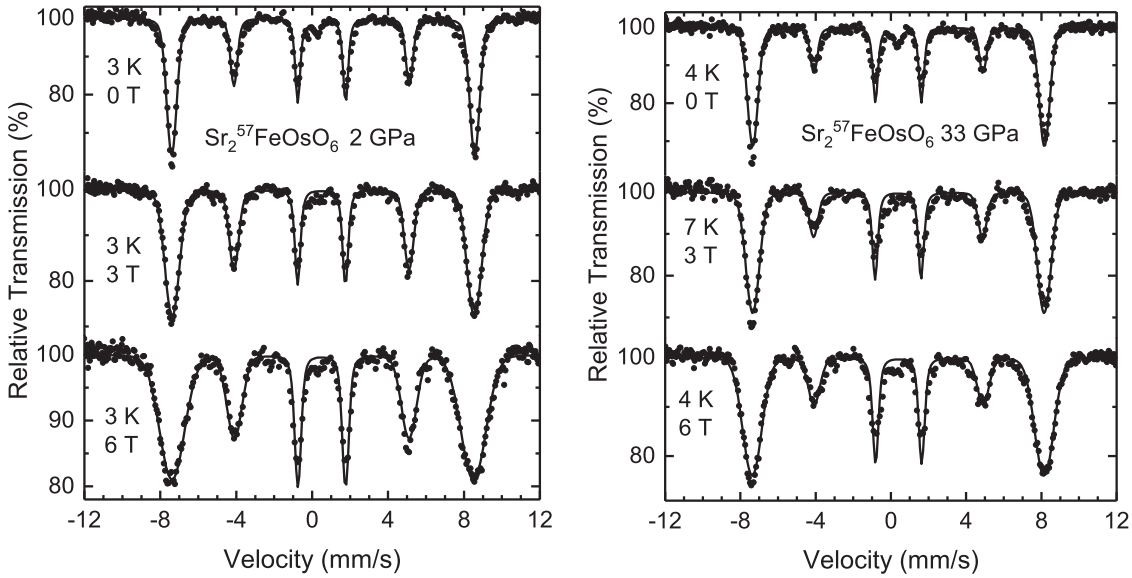

FIG. 8. Dependence of the SMS spectra at 2 and 33 GPa and the lowest temperatures on a longitudinal external magnetic field. The spectra were fitted with a single component having a Gaussian distribution of hyperfine fields.

spectra the separation between the components is arbitrary. Within this analysis the average hyperfine field decreases slightly by about 0.2 T at $B_{ext} = 6$ T for the spectra at 2 GPa, whereas $\langle B_{hf} \rangle$ is independent of B_{ext} within the error limits for the spectra at 33 GPa. The relative intensities of lines 2 and 5 increase slightly at 2 GPa whereas they remain unchanged within the error limits at 33 GPa.

For single-crystal samples, spectra in external fields should allow one to clearly discriminate between the antiferromagnetic (AF) and the ferrimagnetic (FI) spin structures. For AF structures one would expect a splitting of the sextet pattern into two components with hyperfine fields $B_{hf} - B_{ext}$ and $B_{hf} + B_{ext}$, respectively, if B_{ext} would be applied parallel to the easy axis of magnetization, the latter being along the direction of the SMS beam. Furthermore, a spin-flop transition at a critical field $B_{sf} = \sqrt{(2B_E B_A)}$ is anticipated where B_E and B_A are the exchange and anisotropy fields within a mean-field model. For ferrimagnetic Sr_2FeOsO_6 only the Fe sublattice is monitored in the Mössbauer spectra and as all iron moments show parallel spin alignment a shift of the hyperfine pattern by B_{ext}, but no splitting would be expected. Unfortunately, the situation is more complicated in case of powder spectra of antiferromagnets [63] and ferrimagnets [64], where a statistical distribution of the orientations between $\boldsymbol{B}_{ext}$ and the effective field $\boldsymbol{B}_{eff} = \boldsymbol{B}_{hf} + \boldsymbol{B}_{ext}$ occurs. In this case the resulting spectra arise from a superposition of the spectra corresponding to each particular orientation between $\boldsymbol{B}_{eff}$ and $\boldsymbol{B}_{ext}$, and the shape of the spectra sensitively depends on the sizes of B_E and B_A. Furthermore, in the present sample the distribution of orientations is not completely statistical, but preferred orientation effects are apparent. At low temperatures and ambient pressure the spin structure of Sr_2FeOsO_6 is known to be antiferromagnetic [39] and it can be assumed that AF ordering is preserved at 2 GPa. In the spectra at 2 GPa the broadening of the outer lines increases from $B_{ext} = 3$ T to $B_{ext} = 6$ T. This indicates that the spin-flop field is at least about 6 T as for $B_{sf} < 6$ T rather a decreased broadening at 6 T would be anticipated [63]. Thus, a considerable anisotropy field B_A is expected, which is in agreement with the presence of heavy Os atoms where strong spin-orbit coupling leads to a pronounced magnetocrystalline anisotropy. The overall field dependence of the spectra at 33 GPa is similar and no clear signatures for a major pressure-driven change in the spin structure of the iron ions are apparent. Thus, the spectra could be considered as evidence that basically an AF spin structure is retained at high pressures. The line broadening at 6 T is less pronounced than at 2 GPa. This is attributed to an enhanced exchange field B_E and thus to a decreased B_A/B_E ratio as the magnetic exchange interactions are considerably enhanced at high pressure.

Also for FI alignment the shape of powder Mössbauer spectra in an applied field depends on B_E and B_A [64] and in case of pronounced anisotropy also for the FI spin structure strong line broadening for spectra in B_{ext} is anticipated. Thus, the question of the spin structure at high pressure cannot be solved unambiguously from the present powder spectra. However, the proposed AF-FI transition is not the only possible explanation for the evolution of a ferromagnetic signal in the Os $L_{2,3}$ XMCD spectra [42]. An alternative scenario is that high pressure modifies the balance between Fe-Os and Os-Os exchange interactions which could lead to a canting of the spins [62]. A continuous increase of the canting with increasing pressure could explain the continuous evolution of the ferromagnetic Os $L_{2,3}$ signal and rationalize why the size of the ferromagnetic signal even at 40 GPa is still much smaller than for Ca_2FeOsO_6. Another possibility is that the signal corresponds to a minority ferrimagnetic phase which is one of the components constituting the inhomogeneous high-pressure state but which cannot be clearly identified in the Mössbauer spectra.

IV. CONCLUSIONS

We have shown that energy-domain synchrotron ^{57}Fe Mössbauer spectroscopy is a versatile tool to unravel details of the complex magnetism of the double perovskite Sr_2FeOsO_6 at high pressures. The electronic state of iron (Fe^{3+}, $t_{2g}^3 e_g^2$ configuration) remains stable up to the highest applied pressure of about 50 GPa. Broad magnetic hyperfine patterns as well as the coexistence of paramagnetic and magnetically ordered phase are observed over a wide pressure-temperature range. Partly this may reflect a distribution of magnetic ordering temperatures and/or spin-fluctuation times due to residual AS disorder and nonhydrostatic pressure conditions. On the other hand, these effects are also indications for the coexistence of competing magnetic phases arising from the competing exchange interactions within and between the constituent Fe^{3+} and Os^{5+} sublattices. Pronounced changes in the magnetic behavior even at 2 GPa possibly rather reflect the unusual nature of the AF1 phase with partially ordered magnetic moments which still requires further theoretical understanding. The strong enhancement of the magnetic ordering temperature with pressure is in agreement with the behavior expected for a localized Mott-insulating system. Applied-field Mössbauer spectra at low temperature suggest that Sr_2FeOsO_6 basically retains an antiferromagnetic spin structure at high pressures. There are no clear signs which can be attributed to a transformation of the antiferromagnetic into the ferrimagnetic state. The previously reported ferromagnetic response in Os $L_{2,3}$ XMCD spectra under pressure [42] may reflect a progressive spin canting or progressive formation of a minority ferrimagnetic phase, the fraction of which increases continuously with pressure. However, in the latter case the AF-FI transition would extend over a pressure range of several tens of GPa. Theoretical studies on the pressure dependence of the magnetism together with the experimental data may be helpful for discriminating between the various microscopic exchange mechanisms [43,62,65,66] which are believed to govern the magnetism of Sr_2FeOsO_6 and for clarifying the potential role of spin-orbit coupling [50].

ACKNOWLEDGMENTS

We gratefully acknowledge the ESRF for granting beam time at the Nuclear Resonance beamline ID18 for experiment HC-2440. We thank Patrick Merz for synthesizing the ^{57}Fe-enriched Fe_2O_3, Horst Bormann and co-workers for the powder x-ray-diffraction measurement, and Gohil Takur for Rietveld refinement of the XRD data. P.G.N. acknowledges the support by the Russian Science Foundation (Project No. 17-72-20200).

[1] H. G. Drickamer and C. W. Frank, *Electronic Transitions and the High Pressure Chemistry and Physics of Solids*, (Chapman and Hall, London, 1973).

[2] M. Guthrie, Future directions in high-pressure neutron diffraction, J. Phys.: Condens. Matter **27**, 153201 (2015).

[3] G. R. Hearne, M. P. Pasternak, R. D. Taylor, and P. Lacorre, Electronic structure and magnetic properties of $LaFeO_3$ at high pressure, Phys. Rev. B **51**, 11495 (1995).

[4] M. P. Pasternak, R. D. Taylor, R. Jeanloz, X. Li, J. H. Nguyen, and C. A. McCammon, High Pressure Collapse of Magnetism in $Fe_{0.94}O$: Mössbauer Spectroscopy Beyond 100 GPa, Phys. Rev. Lett. **79**, 5046 (1997).

[5] W. M. Xu, O. Naaman, G. Kh. Rozenberg, M. P. Pasternak, and R. D. Taylor, Pressure-induced breakdown of a correlated system: The progressive collapse of the Mott-Hubbard state in $RFeO_3$, Phys. Rev. B **64**, 094411 (2001).

[6] M. Takano, S. Nasu, T. Abe, K. Yamamoto, S. Endo, Y. Takeda, and J. B. Goddenough, Pressure-Induced High-Spin to Low-Spin Transition in $CaFeO_3$, Phys. Rev. Lett. **67**, 3267 (1991).

[7] T. Kawakami, Y. Tsujimoto, H. Kageyama, X-Q. Chen, C. L. Fu, C. Tassel, A. Kitada, S. Suto, K. Hirama, Y. Sekiya, M. Makino, T. Okada, T. Yagi, N. Hayashi, K. Yoshimura, S. Nasu, R. Podloucky, and M. Takano, Spin transition in a four-coordinate iron oxide, Nat. Chem. **1**, 371 (2009).

[8] G. Kh. Rozenberg, W. Xu, and M. P. Pasternak, The Mott insulators at extreme conditions; structural consequences of pressure-induced electronic transitions, Z. Kristallogr. **229**, 210 (2014).

[9] P. Adler, U. Schwarz, K. Syassen, G. Kh. Rozenberg, G. Yu. Machavariani, A. P. Milner, M. P. Pasternak, and M. Hanfland, Collapse of the charge disproportionation and covalency-driven insulator-metal transition in $Sr_3Fe_2O_7$ under pressure, Phys. Rev. B **60**, 4609 (1999).

[10] T. Kawakami, S. Nasu, T. Sasaki, K. Kuzushita, S. Morimoto, S. Endo, T. Yamada, S. Kawasaki, and M. Takano, Pressure-Induced Transition from a Charge-Disproportionated Antiferromagnetic State to a Charge-Uniform Ferromagnetic State in $Sr_{2/3}La_{1/3}FeO_3$, Phys. Rev. Lett. **88**, 037602 (2002).

[11] S. Nasu, High-pressure Mössbauer spectroscopy using synchrotron radiation and radioactive sources, Hyper Interact. **128**, 101 (2000).

[12] G. Kh. Rozenberg, A. P. Milner, M. P. Pasternak, G. R. Hearne, and R. D. Taylor, Experimental confirmation of a p-p intraband gap in Sr_2FeO_4, Phys. Rev. B **58**, 10283 (1998).

[13] S. Medvedev, T. M. Queen, I. A. Troyan, T. Palasyuk, M. I. Eremets, R. J. Cava, S. Naghavi, F. Casper, V. Ksenofontov, G. Wortmann, and C. Felser, Electronic and magnetic phase diagram of β-$Fe_{1.01}Se$ with superconductivity at 36.7 GPa under pressure, Nat. Mater. **8**, 630 (2009).

[14] P. G. Naumov, K. Filsinger, S. I. Shylin, O. I. Barkalov, V. Ksenofontov, Y. Qi, T. Palasyuk, W. Schnelle, S. A. Medvedev, M. Greenblatt, and C. Felser, Pressure-induced magnetic collapse and metallization of $TlFe_{1.6}Se_2$, Phys. Rev. B **96**, 064109 (2017).

[15] H.-J. Hesse, R. Lübbers, M. Winzenick, H. W. Neuling, and G. Wortmann, Pressure and temperature dependence of the Eu valence in $EuNi_2Ge_2$ and related systems studied by Mössbauer effect, X-ray absorption and X-ray diffraction, J. Alloy. Comp. **246**, 220 (1997).

[16] R. Lübbers, G. Wortmann, and H. F. Grünsteudel, High-pressure studies with nuclear scattering of synchrotron radiation, Hyperfine Interact. **123/124**, 529 (1999).

[17] V. Potapkin, L. Dubrovinsky, I. Sergueev, M. Ekholm, I. Kantor, D. Bessas, E. Bykova, V. Prakapenka, R. P. Hermann, R. Rüffer, V. Cerantola, H. J. M. Jönsson, W. Olovsson, S. Mankovsky, H. Ebert, and I. A. Abrikosov, Magnetic interactions in NiO at ultrahigh pressure, Phys. Rev. B **93**, 201110(R) (2016).

[18] G. R. Hearne, M. P. Pasternak, and R. D. Taylor, ^{57}Fe Mössbauer spectroscopy in a diamond-anvil cell at variable high pressures and cryogenic temperatures, Rev. Sci. Instrum. **65**, 3787 (1994).

[19] E. Gerdau, R. Rüffer, H. Winkler, W. Tolksdorf, C. P. Klages, and J. P. Hannon, Nuclear Bragg Diffraction of Synchrotron Radiation in Yttrium Iron Garnet, Phys. Rev. Lett. **54**, 835 (1985).

[20] J. B. Hastings, D. P. Siddons, U. van Bürck, R. Hollatz, and U. Bergmann, Mössbauer Spectroscopy Using Synchrotron Radiation, Phys. Rev. Lett. **66**, 770 (1991).

[21] U. van Bürck, D. P. Siddons, J. B. Hastings, U. Bergmann, and R. Hollatz, Nuclear forward scattering of synchrotron radiation, Phys. Rev. B **46**, 6207 (1992).

[22] G. V. Smirnov, U. van Bürck, A. I. Chumakov, A. Q. R. Baron, and R. Rüffer, Synchrotron Mössbauer source, Phys. Rev. B **55**, 5811 (1997).

[23] T. Mitsui, N. Hirao, Y. Ohishi, R. Masuda, Y. Nakamura, H. Enoki, K. Sakaki, and M. Seto, Development of an energy-domain ^{57}Fe-Mössbauer spectrometer using synchrotron radiation and its application to ultrahigh-pressure studies with a diamond anvil cell, J. Synchrotron Radiat. **16**, 723 (2009).

[24] M. Seto, R. Masuda, S. Higashitaniguchi, S. Kitao, Y. Kobayashi, C. Inaba, T. Mitsui, and Y. Yoda, Synchrotron-Radiation Based Mössbauer Spectroscopy, Phys. Rev. Lett. **102**, 217602 (2009).

[25] P. Gütlich, E. Bill, and A. X. Trautwein, *Mössbauer Spectroscopy and Transition Metal Chemistry* (Springer, Berlin, Heidelberg, 2011), pp. 477–539.

[26] V. Potapkin, A. I. Chumakov, G. V. Smirnov, J.-P. Celse, R. Rüffer, C. McCammon, and L. Dubrovinski, The ^{57}Fe synchrotron Mössbauer source at the ESRF, J. Synchrotron Radiat. **19**, 559 (2012).

[27] V. Potapkin, C. McCammon, K. Glazyrin, A. Kantor, I. Kupenko, C. Prescher, R. Sinmyo, G. V. Smirnov, A. I. Chumakov, R. Rüffer, and L. Dubrovinsky, Effect of iron oxidation state on the electrical conductivity of the Earth's lower mantle, Nat. Commun. **4**, 1427 (2013).

[28] E. Bykova, L. Dubrovinsky, N. Dubrovinskaia, M. Bykov, C. McCammon, S. V. Ovsyannikov, H.-P. Liermann, I. Kupenko, A. I. Chumakov, R. Rüffer, M. Hanfland, and V. Prakapenka, Structural complexity of simple Fe_2O_3 at high pressures and temperatures, Nat. Commun. **7**, 10661 (2016).

[29] I. S. Lyubutin, S. S. Starchikov, A. G. Gavriliuk, I. A. Troyan, Yu. A. Nikiforova, A. G. Ivanova, A. I. Chumakov, and R. Rüffer, Magnetic phase separation and strong enhancement of the Néel temperature at high pressures in a new multiferroic $Ba_3TaFe_3Si_2O_{14}$, JETP. Lett. **105**, 26 (2017).

[30] I. S. Lyubutin, S. S. Starchikov, A. G. Gavriliuk, I. A. Troyan, Yu. A. Nikiforova, A. G. Ivanova, A. I. Chumakov, and

R. Rüffer, High pressure magnetic, structural, and electronic transitions in multiferroic $Ba_3NbFe_3Si_2O_{14}$, Appl. Phys. Lett. **112**, 242405 (2018).

[31] T. Kawakami and S. Nasu, High-pressure Mössbauer spectroscopy of perovskite high valence iron oxides under external magnetic fields, J. Phys.: Condens. Matter **17**, S789 (2005).

[32] S. Vasala and M. Karppinen, $A_2B'B''O_6$ perovskites: A review, Prog. Solid State Chem. **43**, 1 (2015).

[33] K.-I. Kobayasi, T. Kimura, H. Sawada, K. Terakura, and Y. Tokura, Room-temperature magnetoresistance in an oxide material with an ordered double-perovskite structure, Nature (London) **395**, 677 (1998).

[34] Y. Krockenberger, K. Mogare, M. Reehuis, M. Tovar, M. Jansen, G. Vaitheeswaran, V. Kanchana, F. Bultmark, A. Delin, F. Wilhelm, A. Rogalev, A. Winkler, and L. Alff, Sr_2CrOsO_6: End point of a spin-polarized metal-insulator transition by 5*d* band filling, Phys. Rev. B **75**, 020404(R) (2007).

[35] B. Yan, A. K. Paul, S. Kanungo, M. Reehuis, A. Hoser, D. M. Többens, W. Schnelle, R. C. Williams, T. Lancaster, F. Xiao, J. S. Möller, S. J. Blundell, W. Hayes, C. Felser, and M. Jansen, Lattice-Site-Specific Spin Dynamics in Double Perovskite Sr_2CoOsO_6, Phys. Rev. Lett. **112**, 147202 (2014).

[36] R. Morrow, R. Mishra, O. D. Restrepo, M. R. Ball, W. Windl, S. Wurmehl, U. Stockert, B. Büchner, and P. M. Woodward, Independent ordering of two interpenetrating magnetic sublattices in the double perovskite Sr_2CoOsO_6, J. Am. Chem. Soc. **135**, 18824 (2013).

[37] H. L. Feng, S. Calder, M. P. Ghimire, Y.-H. Yuan, Y. Shirako, Y. Tsujimoto, Y. Matsushita, Z. Hu, C.-Y. Kuo, L. H. Tjeng, T.W. Pi, Y.-L. Soo, J. He, M. Tanaka, Y. Katsuya, M. Richter, and K. Yamaura, Ba_2NiOsO_6: A Dirac-Mott insulator with ferromagnetism near 100 K, Phys. Rev. B **94**, 235158 (2016).

[38] H. L. Feng, M. Reehuis, P. Adler, Z. Hu, M. Nicklas, A. Hoser, S-C. Weng, C. Felser, and M. Jansen, Canted ferrimagnetism and giant coercivity in the nonstoichiometric double perovskite $La_2Ni_{1.19}Os_{0.81}O_6$, Phys. Rev. B **97**, 184407 (2018).

[39] A. K. Paul, M. Reehuis, V. Ksenofontov, B. Yan, A. Hoser, D. M. Többens, P. M. Abdala, P. Adler, M. Jansen, and C. Felser, Lattice Instability and Competing Spin Structures in the Double Perovskite Insulator Sr_2FeOsO_6, Phys. Rev. Lett. **111**, 167205 (2013).

[40] R. Morrow, J. R. Soliz, A. J. Hauser, J. C. Gallagher, M. A. Susner, M. D. Sumption, A. A. Aczel, J. Yan, F. Yang, and P. M. Woodward, The effect of chemical pressure on the structure and properties of A_2CrOsO_6 (A = Sr, Ca) ferrimagnetic double perovskite, J. Solid State Chem. **238**, 46 (2016).

[41] H. L. Feng, M. Arai, Y. Matsushita, Y. Tsujimoto, Y. Guo, C. I. Sathish, X. Wang, Y.-H. Yuan, M. Tanaka, and K. Yamaura, High-temperature ferrimagnetism driven by lattice distortion in double perovskite Ca_2FeOsO_6, J. Am. Chem. Soc. **136**, 3326 (2014).

[42] L. S. I. Veiga, G. Fabbris, M. van Veenendaal, N. M. Souza-Neto, H. L. Feng, K. Yamaura, and D. Haskel, Fragility of ferromagnetic double exchange interactions and pressure tuning of magnetism in 3*d*-5*d* double perovskite Sr_2FeOsO_6, Phys. Rev. B **91**, 235135 (2015).

[43] Y. S. Hou, H. J. Xiang, and X. G. Gong, Lattice-distortion induced magnetic transition from low-temperature antiferromagnetism to high-temperature ferrimagnetism in double perovskites A_2FeOsO_6 (A = Ca, Sr), Sci. Rep. **5**, 13159 (2015).

[44] H. L. Feng, P. Adler, M. Reehuis, W. Schnelle, P. Pattison, A. Hoser, C. Felser, and M. Jansen, High-temperature ferrimagnetism with large coercivity and exchange bias in the partially ordered 3*d*/5*d* hexagonal perovskite $Ba_2Fe_{1.12}Os_{0.88}O_6$, Chem. Mater. **29**, 886 (2017).

[45] A. K. Paul, M. Jansen, B. Yan, C. Felser, M. Reehuis, and P. M. Abdala, Synthesis, crystal structure, and physical properties of Sr_2FeOsO_6, Inorg. Chem. **52**, 6713 (2013).

[46] See Supplemental Material at http://link.aps.org/supplemental/10.1103/PhysRevB.99.134443 for further synthetic details and additional structural and Mössbauer data.

[47] Z. Klencsár, A. Kuzmann, and A. Vértes, User-friendly software for Mössbauer spectrum analysis, J. Radioanal. Nucl. Chem. **210**, 105 (1996).

[48] P. Adler, V. Ksenofontov, A. K. Paul, M. Reehuis, B. Yan, M. Jansen, and C. Felser, Magnetic phase transitions and iron valence in the double perovskite Sr_2FeOsO_6, Hyperfine Interact. **226**, 289 (2014).

[49] J. J. Blanco, T. Hernandes, L. M. Rodriguez-Martinez, M. Insausti, J. M. Barandiaran, J.-M. Greneche, and T. Rojo, The effects of Sc and Nb substitution in Sr_2FeReO_6 double perovskites. A combined study of x-ray powder diffraction and Mössbauer spectroscopy, J. Mater. Chem. **11**, 253 (2001).

[50] A. E. Taylor, R. Morrow, M. D. Lumsden, S. Calder, M. H. Upton, A. I. Kolesnikov, M. B. Stone, R. S. Fishman, A. Paramekanti, P. M. Woodward, and A. D. Christianson, Origin of magnetic excitation gap in double perovskite Sr_2FeOsO_6, Phys. Rev. B **98**, 214422 (2018).

[51] I. A. Campbell, S. Senoussi, F. Varret, J. Teillet, and A. Hamzić, Competing Ferromagnetic and Spin-Glass Order in a AuFe Alloy, Phys. Rev. Lett. **50**, 1615 (1983).

[52] R. A. Brand, H. Georges-Gibert, J. Hubsch, and J. A. Heller, Ferrimagnetic to spin glass transition in the mixed spinel $Mg_{1+t}Fe_{2-2t}Ti_tO_4$: A Mössbauer and DC susceptibility study, J. Phys. F: Met. Phys. **15**, 1987 (1985).

[53] W. Kleemann, V. V. Shvartsman, P. Borisov, and A. Kania, Coexistence of Antiferromagnetic and Spin Cluster Glass Order in the Magnetoelectric Relaxor Multiferroic $PbFe_{0.5}Nb_{0.5}O_3$, Phys. Rev. Lett. **105**, 257202 (2010).

[54] S. Chillal, M. Thede, F. J. Litterst, S. N. Gvasaliya, T. A. Shaplygina, S. G. Lushnikov, and A. Zheludev, Microscopic coexistence of antiferromagnetic and spin-glass states, Phys. Rev. B **87**, 220403(R) (2013).

[55] H. L. Feng, Y. Tsujimoto, Y. Guo, Y. Sun, C. I. Sathish, and K. Yamaura, High pressure synthesis, crystal structures, and magnetic properties of the double-perovskite Sr_2FeOsO_6, High Pressure Res. **33**, 221 (2013).

[56] R. Morrow, J. W. Freeland, and P. M. Woodward, Probing the links between structure and magnetism in $Sr_{2-x}Ca_xFeOsO_6$ double perovskites, Inorg. Chem. **53**, 7983 (2014).

[57] E. Granado, J. W. Lynn, R. F. Jardim, and M. S. Torikachvili, Two-Dimensional Magnetic Correlations and Partial Long-Range Order in Geometrically Frustrated Sr_2YRuO_6, Phys. Rev. Lett. **110**, 017202 (2013).

[58] A. P. Ayala, I. Guedes, E. N. Silva, M. S. Augsburger, M. del C. Viola, and J. C. Pedregosa, Raman investigation of A_2CoBO_6

(A = Sr and Ca, B = Te and W) double perovskites, J. Appl. Phys. **101**, 123511 (2007).

[59] R. L. Andrews, A. M. Heyns, and P. M. Woodward, Raman studies on A_2MWO_6 tungstate double perovskites, Dalton Trans. **44**, 10700 (2015).

[60] B. Manoun, J. M. Igartua, P. Lazor, and A. Ezzahi, High temperature induced phase transitions in Sr_2ZnWO_6 and Sr_2CoWO_6 double perovskite oxides: Raman spectroscopy as a tool, J. Mol. Struct. **1029**, 81 (2012).

[61] V. A. Sarkisyan, I. A. Troyan, I. S. Lyubutin, A. G. Gavrilyuk, and A. F. Kashuba, Magnetic collapse and the change of electronic structure of $FeBO_3$ antiferromagnet under pressure, JETP. Lett. **76**, 664 (2002).

[62] O. N. Meetei, O. Erten, M. Randeria, N. Trivedi, and P. Woodward, Theory of High T_C Ferrimagnetism in a Multiorbital Mott Insulator, Phys. Rev. Lett. **110**, 087203 (2013).

[63] Q. A. Pankhurst and R. J. Pollard, Mössbauer spectra of antiferromagnetic powders in applied fields, J. Phys.: Condens. Matter **2**, 7329 (1990).

[64] Q. A. Pankhurst, Anisotropy field measurement in barium ferrite powders by applied field Mössbauer spectroscopy, J. Phys.: Condens. Matter **3**, 1323 (1991).

[65] S. Kanungo, B. Yan, M. Jansen, and C. Felser, Ab *initio* study of low-temperature magnetic properties of double perovskite Sr_2FeOsO_6, Phys. Rev. B **89**, 214414 (2014).

[66] K. Samanta and T. Saha-Dasgupta, Comparative study of electronic structure and magnetic properties of osmate double perovskites: Ca_2FeOsO_6 versus $Ca_2Co(Ni)OsO_6$, J. Phys. Soc. Jpn. **87**, 041007 (2018).